New Uranium Chalcoantimonates, RbU_2SbS_8 and KU_2SbSe_8, with a Polar Noncentrosymmetric Structure

Kyoung-Shin Choi and Mercouri G. Kanatzidis*

Department of Chemistry and Center for Fundamental Materials Research, Michigan State University, East Lansing, Michigan 48824

Received May 21, 1999

The new compounds, RbU_2SbS_8 and KU_2SbSe_8, were prepared as golden-black, blocklike crystals by the polychalcogenide molten flux method. RbU_2SbS_8 crystallizes in the monoclinic space group *Cm* with $a = 7.9543(9)$ Å, $b = 11.0987(13)$ Å, $c = 7.2794(10)$ Å, $\beta = 106.030(2)°$, and $Z = 2$. The compound has a two-dimensional character with layers running perpendicular to the *c*-axis. The coordination geometry around the U^{4+} atoms is best described as a bicapped trigonal prism. The trigonal prisms share triangular faces with neighboring prisms, forming one-dimensional columns along the *a*-axis. The columns are then joined to construct sheets by sharing capping S atoms. Sb^{3+} ions are sitting at the center of a slightly distorted seesaw coordination environment (CN = 4). Rb^+ ions are stabilized in 8-coordinate bicapped trigonal prismatic sites. KU_2SbSe_8 crystallizes in the monoclinic space group *Cm* with $a = 11.5763(2)$ Å, $b = 8.2033(1)$ Å, $c = 15.2742(1)$ Å, $\beta = 112.22(2)°$, and $Z = 4$. KU_2SbSe_8 has essentially the same structure as RbU_2SbS_8. However, Sb^{3+} and K^+ ions appear disordered in every other layer, resulting in a different unit cell. RbU_2SbS_8 is a semiconductor with a band gap of 1.38 eV. The band gap of KU_2SbSe_8 could not be determined precisely due to the presence of overlapping intense f−f transitions in the region (0.5−1.1 eV). The Raman spectra show the disulfide stretching vibration in RbU_2SbS_8 at 479 cm^{-1} and the diselenide stretching vibration in KU_2SbSe_8 at 252 cm^{-1}. Magnetic susceptibility measurements indicate the presence of U^{4+} centers in the compounds. The compounds do not melt below 1000 °C under vacuum.

1. Introduction

For the past few years, we have been investigating chalcoantimonate compounds, with rare earth or actinide metals. The molten polychalcogenide flux method has been essential for this type of exploration and resulted in several new selenoantimonates such as $KThSb_2Se_6$,[1] $K_2Gd_2Sb_2Se_9$,[2] and $EuSbSe_3$.[3] Due to the large size of the f-elements, the bonding between the metals and the chalcogen atoms is primarily ionic in character and the coordination sphere is large and flexible. This property, when combined with the property of Sb^{3+} ions to have stereochemically active lone pairs, increases the chances to produce unique structure types in these compounds. Recently, the reaction of A_x-Sb_yQ_z (A = Rb, K; Q = S, Se) flux with uranium metal yielded new compounds RbU_2SbS_8 and KU_2SbSe_8, which present a unique polar noncentrosymmetric arrangement of atoms. Compounds with noncentrosymmetric structures are of considerable interest due to their potential applications as piezoelectrics, ferroelectrics, and nonlinear optics.[4] To date, only a few quaternary uranium chalcogenide compounds are known (e.g., $Rb_4U_4P_4Se_{26}$,[5] $K_2UP_3Se_9$,[6] $CsTiUTe_5$,[7] $CsCuUTe_3$,[7] $Cs_8Hf_5UTe_{30.6}$,[8] and $KCuUSe_3$[9]), and none of them has a noncentrosymmetric structure. Here we report the synthesis, structural and physicochemical characterization of RbU_2SbS_8 and KU_2SbSe_8.

2. Experimental Section

2.1. Synthesis. The following reagents were used as obtained: uranium, 99.7%, −60 mesh, Cerac, Milwaukee, WI; antimony, 99.999%, −200 mesh, Cerac, Milwaukee, WI; selenium powder, 99.95%, −200 mesh, Cerac Inc., Milwaukee, WI; sulfur powder, sublimed, JT Baker Co., Philllipsberg, NJ; rubidium metal, 99.8%, Johnson Matthey Co., Ward Hill, MA; potassium metal, granules, <6 mm, 99% purity, Aldrich Chemical Co., Inc., Milwaukee, WI. The K_2Se/Rb_2S starting materials were prepared by a stoichiometric reaction of potassium/rubidium metal and selenium/sulfur in liquid NH_3.

RbU_2SbS_8. This compound was synthesized from a mixture of 0.0633 g (0.3 mmol) of Rb_2S, 0.0714 g (0.3 mmol) of U, 0.0366 g (0.3 mmol) of Sb, and 0.0867 g (2.7 mmol) of S. The reagents were thoroughly mixed, sealed in an evacuated quartz ampule, and heated at 650 °C for 5 days (cooling 2 °C/h). Pure reddish black, blocklike crystals of RbU_2SbS_8 were obtained by isola-

(1) Choi, K.-S.; Iordanidis, L.; Chondroudis, K.; Kanatzidis, M. G. *Inorg. Chem.* **1997**, *36*, 3804−3805.
(2) Choi, K.-S.; Hanko, J. A.; Kanatzidis, M. G. *J. Solid State Chem.* in press.
(3) Choi, K.-S.; Kanatzidis, M. G. Manuscript in preparation.
(4) (a) West, A. R. *Solid State Chemistry and Its Applications*; John Wiley & Sons: New York, 1984; pp 540−552. (b) Xia, Y.; Chen, C.; Tang, D.; Wu, B. *Adv. Mater.* **1995**, *7*, 79−81.
(5) Chondroudis, K.; Kanatzidis, M. G. *J. Am. Chem. Soc.* **1997**, *119*, 2574−2575.
(6) Chondroudis, K.; Kanatzidis, M. G. *C. R. Acad. Sci., Ser. B* **1996**, *322*, 887−894.
(7) Cody, J. A.; Ibers, J. A. *Inorg. Chem.* **1995**, *34*, 3165−3172.
(8) Cody, J. A.; Mansuetto, M. F.; Pell, M. A.; Chien, S.; Ibers, J. A. *J. Alloys Compd.* **1995**, *219*, 59−62.
(9) Sutorik, A. C.; Albritton-Thomas, J.; Hogan, T.; Kannewurf, C. R.; Kanatzidis, M. G. *Chem. Mater.* **1996**, *8*, 751−761.

10.1021/cm990320l CCC: $18.00
Published on Web 08/27/1999

Table 1. Summary of Crystallographic Data and Structural Analysis for RbU_2SbS_8 and KU_2SbSe_8

	RbU_2SbS_8	RbU_2SbS_8	KU_2SbSe_8	KU_2SbSe_8
fw	939.76	939.76	1268.59	1268.59
cryst habit	reddish black blocks		golden-black blocks	
space group	*Amm*2	*Cm*	*Amm*2	*Cm*
a, Å	5.551(1)	7.9543(9)	5.7811(8)	11.5763(2)
b, Å	3.978(2)	11.099(1)	4.0988(5)	8.2033(1)
c, Å	14.057(5)	7.279(1)	14.184(2)	15.2742(1)
β, deg	90	106.030(2)	90	112.22(2)
Z; *V*, Å^3	1; 310.4(2)	2; 617.7(1)	1; 336.10(8)	4; 1342.75(3)
D_{calcd}, g/cm^3	5.028	5.053	6.268	6.275
temp, K	298(2)	170(2)	298(2)	170(2)
λ(Mo Kα), Å	0.71073	0.71073	0.71073	0.71073
μ(Mo Kα), cm^{-1}	333.71	335.38	479.47	480.06
F(000)	400	800	526	2104
θ_{max}, deg	24.75	28.26	25.02	28.20
tot. no. of data measd	1096	2843	882	5255
no of unique data	348	1252	266	3031
	(R_{int} = 0.066)	(R_{int} = 0.050)	(R_{int} = 0.055)	(R_{int} = 0.045)
no. of variables	26	63	26	132
refinement method	full-matrix least-squares on F^2			
final *R* indices [$I > 2\sigma$]	R1[a] = 0.0580	R1 = 0.0290	R1 = 0.0355	R1 = 0.0577
	WR2[b] = 0.1408	wR2 = 0.0697	wR2 = 0.0904	wR2 = 0.1839
R indices (all data)	R1 = 0.0580	R1 = 0.0294	R1 = 0.0355	R1 = 0.0724
	wR2 = 0.1408	wR2 = 0.0700	wR2 = 0.0904	wR2 = 0.2006
GOF on F^2	1.239	1.073	1.157	1.137
BASF	0.54(4)	0.52(1)	0.44(4)	0.76(2)

[a] $R1 = \sum||F_o| - |F_c||/\sum|F_o|$. [b] $wR2 = \{\sum[w(F_o^2 - F_c^2)^2]/\sum[w(F_o^2)^2]\}^{1/2}$.

tion in degassed dimethylformamide (DMF) and water (yield >90% based on U metal). The crystals are air and water stable.

KU_2SbSe_8. This compound was synthesized from a mixture of 0.0471 g (0.3 mmol) of K_2Se, 0.0714 g (0.3 mmol) of U, 0.0366 g (0.3 mmol) of Sb, and 0.2132 g (2.7 mmol) of Se. The reagents were thoroughly mixed, sealed in an evacuated quartz ampule, and heated at 650 °C for 5 days (cooling 2 °C/h). Pure golden black, blocklike crystals of KU_2SbSe_8 were obtained by isolation in degassed dimethylformamide (DMF) and water (yield >90% based on U metal). The crystals are air and water stable.

The compositions of the materials were analyzed by scanning electron microscope (SEM)/energy dispersive spectroscopy (EDS). Homogeneity for both compounds was confirmed by comparing the powder X-ray diffraction patterns of the products against ones calculated using X-ray single-crystal data.

2.2. Physical Measurements. Solid-State UV/Vis Spectroscopy. Optical diffuse reflectance measurements were performed at room temperature with a Shimadzu UV-3101 PC double-beam, double-monochromator spectrophotometer operating in the 200−2500 nm region. The instrument is equipped with an integrating sphere and is controlled by a personal computer. $BaSO_4$ was used as a 100% reflectance standard for all materials. Samples were prepared by grinding them to a fine powder, spreading them on a compacted surface of the powdered standard material and preloading them into a sample holder. The reflectance vs wavelength data generated were used to estimate a material's band gap by converting reflectance to absorption data as described previously.[10]

Magnetic Susceptibility. The magnetic susceptibilities for RbU_2SbS_8 and KU_2SbSe_8 were measured over the range 2−300 K using a MPMS Quantum Design SQUID magnetometer. The sample was ground to a fine powder to minimize possible anisotropic effects and loaded into PVC containers. The temperature-dependent susceptibility studies were performed at 1000 G. Corrections for the diamagnetism of the sample containers were made by measuring the magnetic response of the empty container under the same conditions of temperature and field which were measured for the filled container. Diamagnetic contribution of every ion to χ_M was corrected according to Selwood.[11]

Differential Thermal Analysis (DTA). DTA experiments were performed on a computer-controlled Shimadzu DTA-50 thermal analyzer. Typically a sample (~20 mg) of ground crystalline material was sealed in quartz ampules under vacuum. A quartz ampule of equal mass filled with Al_2O_3 was sealed and placed on the reference side of the detector. The samples were heated to 800 °C at 5 °C/min and then isothermed for 10 min followed by cooling at −5 °C/min to 50 °C. Residues of the DTA experiments were examined by X-ray powder diffraction. The stability/reproducibility of the samples was monitored by running multiple heating/cooling cycles.

Raman Spectroscopy. Raman spectra were recorded on a Holoprobe Raman spectrograph equipped with a CCD camera detector using 633 nm radiation from a HeNe laser for excitation. Laser power at the sample was estimated to be about 5 mW, and the focused laser beam diameter was ca. 10 μm. A total of 5 scans were needed to obtain good quality spectra. The accumulation time of each scan was 50 s.

2.3. X-ray Crystallography. Single crystals of RbU_2SbS_8 with dimensions 0.28 × 0.13 × 0.10 mm and of KU_2SbSe_8 with dimensions of 0.12 × 0.10 × 0.04 mm were mounted on the tip of a glass fiber. Intensity data for RbU_2SbS_8 were collected at room temperature on a Rigaku AFC6S four circle automated diffractometer equipped with a graphite-crystal monochromator. The unit cell parameters were determined from a least-squares refinement using the setting angles of 20 carefully centered reflections in the 8° < 2θ < 30° range. The data were collected with the ω-scan technique over a full sphere of reciprocal space, up to 50° in 2θ. Crystal stability was monitored with three standard reflections whose intensities were checked every 150 reflections. No significant decay was observed during the data collection period. An empirical absorption correction was applied based on ψ scans.

Intensity data for KU_2SbSe_8 were collected at room temperature on a Siemens SMART Platform CCD diffractometer using graphite-monochromatized Mo Kα radiation. The data were collected over a full sphere of reciprocal space, up to 50.04° in 2θ. The individual frames were measured with an omega rotation of 0.3° and an acquisition time of 30 s. The SMART[12] software was used for the data acquisition and SAINT[13] for the data extraction and reduction. The absorption correction was performed using SADABS.[14] The complete data

(10) McCarthy, T. J.; Ngeyi, S.-P.; Liao, J.-H.; Degroot, D.; Hogan, T.; Kannewurf, C. R.; Kanatzidis, M. G. *Chem. Mater.* **1993**, *5*, 331.

(11) Selwood, P. W. *Magnetochemistry*, 2nd ed.; Interscience Publishers: New York, 1956.

(12) SMART: Siemens Analytical Xray Systems, Inc.: Madison, WI, 1994.

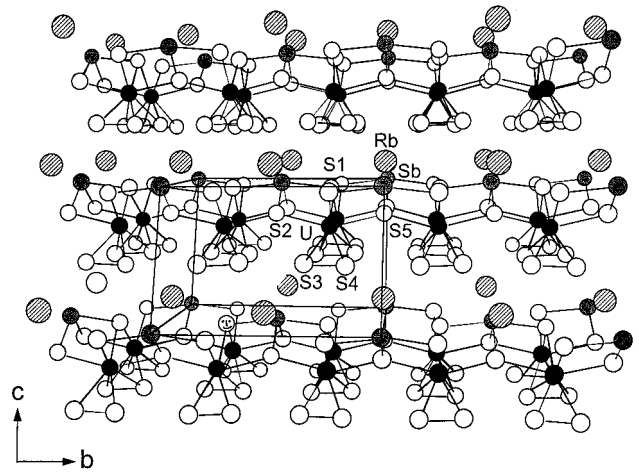

Figure 1. Structure of RbU_2SbS_8 (*Cm*) viewed down the *a*-axis.

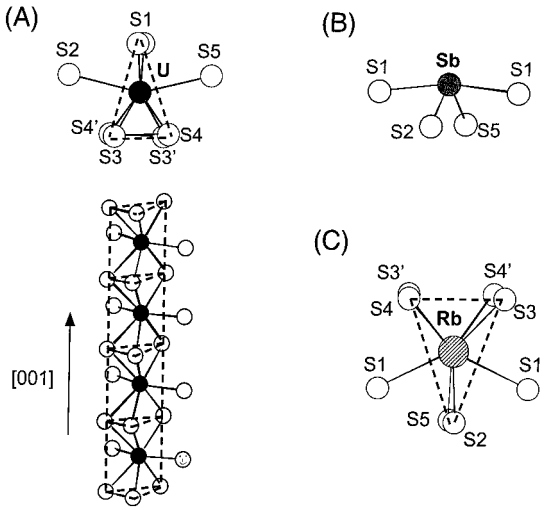

Figure 2. Coordination environment of (A) the U atoms and the one-dimensional columns along the *a*-axis, (B) the Sb atoms, and (C) the Rb atoms.

collection parameters and details of the structure solution and refinement for both compounds are given in Table 1.

Structure solution and refinement for both compounds were performed with the SHELXTL package of crystallographic programs.[15] Systematic absence conditions of the data sets gave four possible space groups, *Cmmm*, *Cmm*2, *Amm*2, *C*222. The structures were solved and refined successfully in the polar *Amm*2 space group. Due to the absence of mirror planes perpendicular to the *c*-axis, these structures are clearly polar and could not be solved in the centrosymmetric space group *Cmmm*. All the crystals used for the structure solution were racemically twinned, and the BASF parameters were refined. In RbU_2SbS_8, the Sb^{3+} and Rb^+ sites were half-occupied and the distance between them was 0.92 Å, indicating that only one of the ions is present at a time with a probability of 50%. KU_2SbSe_8 showed the same disorder pattern between the Sb^{3+} and K^+ ions. These results suggest that there may exist a supercell which could resolve the disorder.

Intensity data for both compounds were recollected on a Siemens SMART Platform CCD diffractometer with better grown crystals and a longer acquisition time of 70 s per frame

(13) SAINT: Version 4; Siemens Analytical Xray Systems, Inc.: Madison, WI, 1994−1996.

(14) Sheldrick, G. M. University of Göttingen, Germany. To be published.

(15) SHELXTL: Version 5, Sheldrick, G. M. Siemens Analytical Xray Systems, Inc.: Madison, WI, 1994.

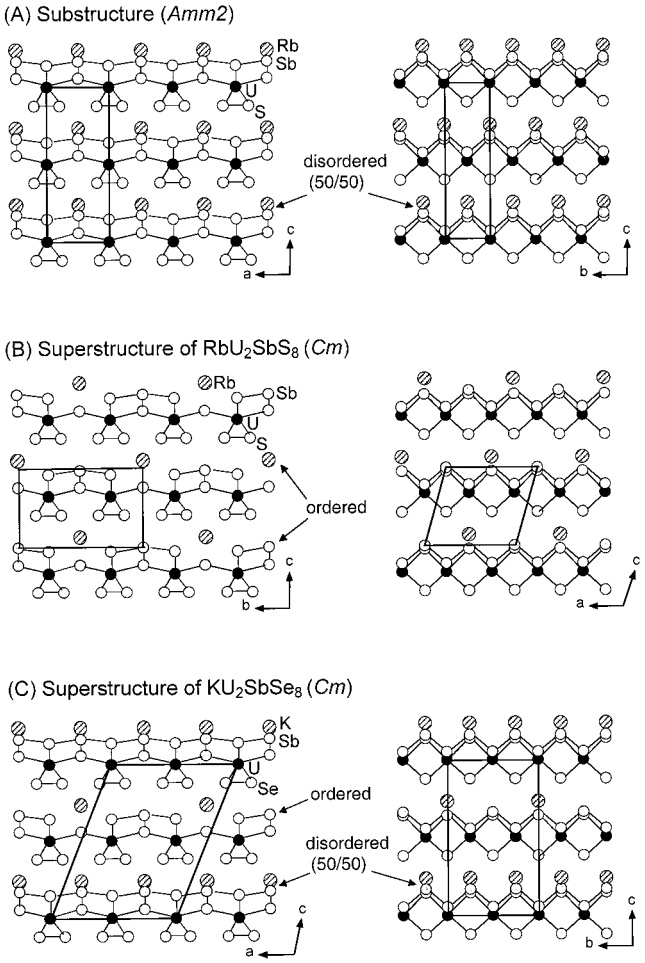

Figure 3. Schematic comparison of the ordering and disordering patterns of Sb^{3+} and Rb^+/K^+ in (A) the substructure, (B) the superstructure of RbU_2SbS_8, and (C) the superstructure of KU_2SbSe_8.

to probe the existence of a superstructure. It was indeed found that RbU_2SbS_8 and KU_2SbSe_8 possess monoclinic supercells. Interestingly, the supercells are different for each compound. The vectorial relationships between the supercell parameters, *a*′, *b*′, and *c*′ and the subcell parameters, *a*, *b*, *c* for each compound are as follows:

$$RbU_2SbS_8: \quad a' = 2b \quad b' = -2a \quad c' = -0.5b + 0.5c$$

$$KU_2SbSe_8: \quad a' = 2a \quad b' = 2b \quad c' = -a + c$$

The complete data collection parameters and details of the structure solutions and refinements are given in Table 1.

Both superstructures were solved and refined successfully in the polar *Cm* space group. The fact that RbU_2SbS_8 and KU_2SbSe_8 were solved in the same space group is coincidental as they have different unit cells and different monoclinic *b*-axes. Again both of the superstructures are clearly polar (see Figures 1 and 4) and could not be solved in the centrosymmetric space group *C*2/*m*.

The coordinates of all atoms, isotropic temperature factors, and their estimated standard deviations (esd's) for RbU_2SbS_8 and KU_2SbSe_8 are given in Tables 2 and 3, respectively. The selected bond distances and angles are given in Tables 4 and 5.

3. Results and Discussion

Structures. As shown in Figure 1, RbU_2SbS_8 has a two-dimensional character with layers running perpen-

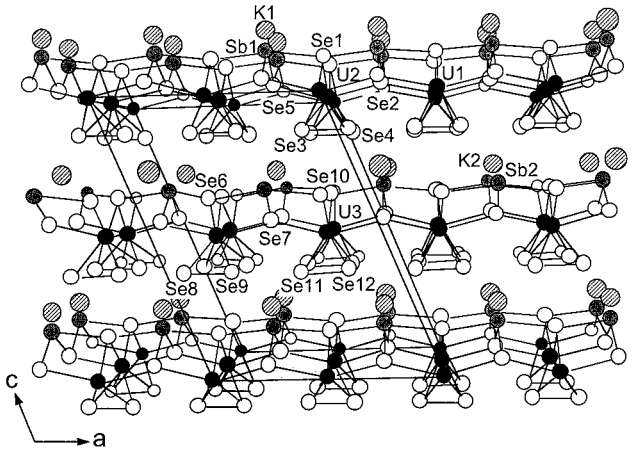

Figure 4. Structure of KU_2SbSe_8 (*Cm*) viewed down the *b*-axis.

Table 2. Fractional Atomic Coordinates and Equivalent Isotropic Displacement Parameter Values for RbU_2SbS_8 (*Cm*) with Estimated Standard Deviations in Parentheses

atom	*x*	*y*	*z*	*U*(eq),[a] Å^2
U(1)	0.3298(1)	2498(1)	0.3126(2)	0.005(1)
Sb(1)	0.0000(1)	0	0.0000(2)	0.008(1)
Rb(1)	0.4596(2)	0	0.8420(2)	0.009(1)
S(1)	0.0097(5)	2404(2)	0.0422(5)	0.008(1)
S(2)	0.2952(5)	0	0.2165(6)	0.009(1)
S(3)	0.1346(4)	0.1637(3)	0.5565(5)	0.010(1)
S(4)	0.1406(4)	0.3523(2)	0.5444(5)	0.010(1)
S(5)	0.8125(5)	0	0.2148(6)	0.009(1)

[a] *U*(eq) is defined as one-third of the trace of the orthogonalized $\mathbf{U}_{ij}$ tensor.

Table 3. Fractional Atomic Coordinates and Equivalent Isotropic Displacement Parameter Values for KU_2SbSe_8 (*Cm*) with Estimated Standard Deviations in Parentheses

atom	*x*	*y*	*z*	*U*(eq), Å^2
U(1)	0.4990(1)	0	0(1)	0.009(1)
U(2)	0.0000(1)	0	0(1)	0.009(1)
U(3)	0.2493(1)	0.2500(1)	0.5000(1)	0.009(1)
Sb(1)	0.3337(4)	0.2495(22)	0.1618(3)	0.017(1)
Sb(2)	0.5788(3)	0	0.6644(3)	0.012(1)
K(1)	0.3692(13	0.2460(22)	0.2336(9)	0.017(1)
K(2)	0.1128(7)	0	0.7327(6)	0.016(1)
Se(1)	0.0692(3)	0.2500(2)	0.1402(2)	0.013(1)
Se(2)	0.2743(3)	0	0.0498(3)	0.013(1)
Se(3)	0.3341(2)	0.2544(2)	0.8745(2)	0.014(1)
Se(4)	0.0400(3)	0.2550(3)	0.8765(2)	0.015(1)
Se(5)	0.7746(3)	0	0.0502(3)	0.013(1)
Se(6)	0.3261(3)	0	0.6407(3)	0.011(1)
Se(7)	0.0251(2)	0.2511(2)	0.5512(2)	0.014(1)
Se(8)	0.0820(3)	0	0.3779(3)	0.017(1)
Se(9)	0.2832(3)	0	0.3736(2)	0.014(1)
Se(10)	0.8131(3)	0	0.6412(3)	0.014(1)
Se(11)	0.5894(3)	0	0.3754(2)	0.015(1)
Se(12)	0.7930(3)	0	0.3756(2)	0.014(1)

dicular to the *c*-axis. The uranium atoms occupy the center of a bicapped trigonal prism of S atoms made of two $(S_2)^{2-}$ units forming the two short parallel edges of the prism, and four S^{2-} ions at the apex and capping positions. The S−S distance in the disulfide group is normal at 2.096(5) Å.[2,16] The formula can therefore be written as $Rb^+U^{4+}{}_2Sb^{3+}(S^{2-})_4(S_2)^{2-}{}_2$. The U^{4+}-centered trigonal prism shares its triangular faces with neighboring prisms along the *a*-axis forming one-dimensional columns, which are similar to those found in $ZrSe_3$;[16] see Figure 2A. Then, these columns are connected side

(16) Furuseth, S.; Brattas, L.; Kjekshus, A. *Acta Chem. Scand.* **1975**, *A29*, 623−631.

Table 4. Selected Distances (Å) and Bond Angles (deg) for RbU_2SbS_8 (*Cm*)

Bond Distances			
U(1)−S(1)	2.737(4)	Rb(1)−S(1)	3.203(3) × 2
U(1)−S(3)	2.752(3)	Rb(1)−S(5)	3.322(4)
U(1)−S(1)	2.757(3)	Rb(1)−S(2)	3.333(5)
U(1)−S(4)	2.795(3)	Rb(1)−S(4)	3.343(4) × 2
U(1)−S(4)	2.818(3)	Rb(1)−S(3)	3.367(3) × 2
U(1)−S(3)	2.829(3)	Sb(1)−S(2)	2.440(4)
U(1)−S(2)	2.854(1)	Sb(1)−S(5)	2.441(5)
U(1)−S(5)	2.861(1)	Sb(1)−S(1)	2.684(2) × 2
S(3)−S(4)	2.096(5)		

Bond Angles			
S(1)−U(1)−S(3)	84.71(10)	S(2)−Sb(1)−S(5)	103.6(2)
S(1)−U(1)−S(1)	92.93(12)	S(2)−Sb(1)−S(1)	86.21(8)
S(1)−U(1)−S(4)	153.36(8)	S(5)−Sb(1)−S(1)	86.00(9)
S(3)−U(1)−S(4)	89.64(9)	S(5)−Sb(1)−S(1)	86.00(9)
S(4)−U(1)−S(4)	109.38(12)	S(1)−Sb(1)−S(1)	167.4(2)
S(3)−U(1)−S(3)	104.55(11)	S(1)−Rb(1)−S(1)	128.17(13)
S(4)−U(1)−S(3)	43.77(11)	S(1)−Rb(1)−S(5)	69.97(7)
S(1)−U(1)−S(2)	84.07(10)	S(5)−Rb(1)−S(2)	76.46(11)
S(3)−U(1)−S(2)	120.35(10)	S(1)−Rb(1)−S(4)	135.54(11)
S(4)−U(1)−S(2)	120.78(11)	S(5)−Rb(1)−S(4)	96.39(9)
S(3)−U(1)−S(2)	78.05(11)	S(2)−Rb(1)−S(4)	150.05(6)
S(1)−U(1)−S(5)	77.37(10)	S(1)−Rb(1)−S(4)	80.33(9)
S(4)−U(1)−S(5)	75.99(11)	S(4)−Rb(1)−S(4)	58.71(11)
S(3)−U(1)−S(5)	119.14(11)	S(5)−Rb(1)−S(3)	146.69(6)
S(2)−Rb(1)−S(3)	95.57(9)		
S(4)−Rb(1)−S(3)	105.02(10)		

Table 5. Selected Distances (Å) and Bond Angles (deg) for KU_2SbSe_8(*Cm*)

Bond Distances			
U(1)−Se(1)	2.852(3) × 2	Sb(1)−Se(2)	2.588(14)
U(1)−Se(4)	2.917(2) × 2	Sb(1)−Se(5)	2.591(14)
U(1)−Se(2)	2.973(3)	Sb(1)−Se(1)	2.868(5)
U(1)−Se(3)	2.984(2) × 2	Sb(1)−Se(1)	2.952(5)
U(1)−Se(5)	2.987(3)	Sb(2)−Se(7)	2.594(3) × 2
U(2)−Se(1)	2.852(3) × 2	Sb(2)−Se(6)	2.809(4)
U(2)−Se(3)	2.939(2) × 2	Sb(2)−Se(10)	2.866(5)
U(2)−Se(4)	2.969(2) × 2	K(1)−Se(1)	3.147(14)
U(2)−Se(2)	2.972(3)	K(1)−Se(1)	3.216(14)
U(2)−Se(5)	2.984(3)	K(1)−Se(2)	3.29(2)
U(3)−Se(6)	2.859(3)	K(1)−Se(5)	3.33(2)
U(3)−Se(10)	2.863(3)	K(1)−Se(11)	3.33(2)
U(3)−Se(11)	2.931(2)	K(1)−Se(8)	3.34(2)
U(3)−Se(9)	2.943(2)	K(1)−Se(9)	3.35(2)
U(3)−Se(8)	2.950(3)	K(1)−Se(12)	3.36(2)
U(3)−Se(12)	2.965(2)	K(2)−Se(10)	3.213(9)
U(3)−Se(7)	2.980(3)	K(2)−Se(6)	3.271(8)
U(3)−Se(7)	2.987(3)	K(2)−Se(7)	3.292(7) × 2
Se(3)−Se(4)	2.375(4)	K(2)−Se(4)	3.362(6) × 2
Se(8)−Se(9)	2.356(5)	K(2)−Se(3)	3.378(7) × 2
Se(11)−Se(12)	2.356(5)		

Bond Angles			
Se(1)−U(1)−Se(1)	91.95(11)	Se(2)−Sb(1)−Se(5)	104.7(2)
Se(1)−U(1)−Se(4)	155.68(8)	Se(2)−Sb(1)−Se(1)	87.2(3)
Se(4)−U(1)−Se(4)	87.13(10)	Se(5)−Sb(1)−Se(1)	87.1(3)
Se(1)−U(1)−Se(2)	80.61(8)	Se(2)−Sb(1)−Se(1)	85.5(3)
Se(4)−U(1)−Se(2)	122.54(7)	Se(5)−Sb(1)−Se(1)	85.5(3)
Se(1)−U(1)−Se(3)	156.44(9)	Se(1)−Sb(1)−Se(1)	167.9(2)
Se(4)−U(1)−Se(3)	47.44(8)	Se(1)−K(1)−Se(1)	130.9(4)
Se(2)−U(1)−Se(3)	75.83(8)	Se(1)−K(1)−Se(5)	71.1(3)
Se(3)−U(1)−Se(3)	88.74(9)	Se(1)−K(1)−Se(11)	136.7(6)
Se(1)−U(1)−Se(5)	80.42(8)	Se(2)−K(1)−Se(11)	96.3(4)
Se(4)−U(1)−Se(5)	75.30(8)	Se(5)−K(1)−Se(11)	148.7(5)
Se(2)−U(1)−Se(5)	152.57(12)	Se(1)−K(1)−Se(8)	133.6(5)
Se(3)−U(1)−Se(5)	121.78(7)	Se(2)−K(1)−Se(8)	150.5(5)
Se(5)−K(1)−Se(8)	95.2(5)		
Se(11)−K(1)−Se(8)	75.9(3)		
Se(8)−K(1)−Se(9)	106.1(4)		
Se(2)−K(1)−Se(12)	147.9(5)		
Se(5)−K(1)−Se(12)	94.1(4)		

by side sharing S^{2-} atoms on the capping sites to build two-dimensional layers.

The Sb^{3+} atoms are at the center of a slightly distorted seesaw coordination environment[17] (CN = 4), allowing its $5s^2$ lone pair to fully express itself; see Figure 2B. Rb^+ ions are stabilized in a basically identical environment as the Sb^{3+} ions. However, instead of sitting at the center of the seesaw, they move up toward the middle of interlayer space in order to be coordinated by four more S atoms from the upper layer. Thus, they are stabilized in 8-coordinate bicapped trigonal prismatic sites; see Figure 2C.

The difference between the substructure and the superstructure of RbU_2SbS_8 lies only in the ordering pattern of the Sb^{3+} and Rb^+ cations. While the substructure shows an apparent 50/50 statistical disorder between the Rb and Sb ions, the superstructure resolves this disorder and presents a periodic arrangement of these ions along all the axes. The uranium−chalcogen framework in the superstructure remains the same as in the substructure. Figure 3 shows a schematic comparison of the cationic arrangement in the substructure and the superstructure of RbU_2SbS_8.

The structure of KU_2SbSe_8 (supercell description) is slightly different from that of RbU_2SbS_8 in that the Sb^{3+} and K^+ ions are well-ordered only in every other layer and disordered in the remaining layers; see Figure 3C and Figure 4. At this point, it is not certain if the Sb^{3+} and K^+ ions are really disordered in every other layer or if this observation is again an artifact caused by the existence of yet a larger supercell that can remove this disorder. We did indeed observe additional supercell reflections which would double the supercell axis perpendicular to the layer: a = 8.183(2) Å, b = 11.546(3) Å, c = 56.42(1) Å, $\alpha = 90.0°$, $\beta = 90.0°$, and $\gamma = 90.0°$. However, these reflections were extremely weak, and we could not collect enough data to precisely probe this additional superstructure. Increasing the acquisition time per frame to longer than 80 s did not improve the quality of the data. In any case, this suggests that the disorder between the K^+ and Sb^{3+} ions is probably a crystallographic artifact.

Properties. These materials are valence-precise and are expected to be semiconductors. Indeed, RbU_2SbS_8 shows an abrupt optical gap at 1.38 eV; see Figure 5. The spectrum also shows intense absorption bands at 0.52, 0.75, and 1.02 eV, which can be associated with the f−f transitions as observed in other compounds with U^{4+} ions.[18]

The band gap of KU_2SbSe_8, which appears to be around 0.6 eV, could not be defined precisely because the absorption edge is interfered with by the f−f transitions, which exist at the same energy as RbU_2SbS_8. The f−f transitions are not usually affected by external influences such as changing the ligands from S to Se because the f orbitals are well shielded by the s and p orbitals.

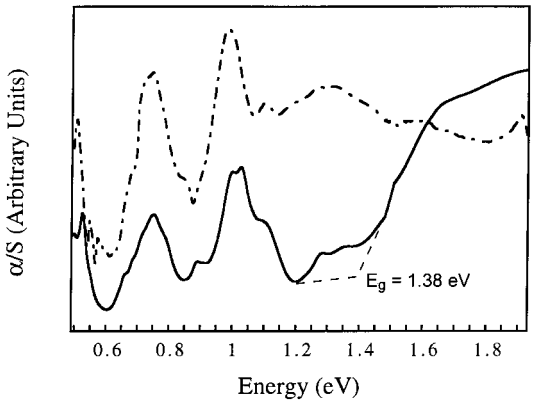

Figure 5. Optical absorption spectrum of RbU_2SbS_8 (—) and KU_2SbSe_8 (-·-). The band gap value, E_g, is shown in the figure.

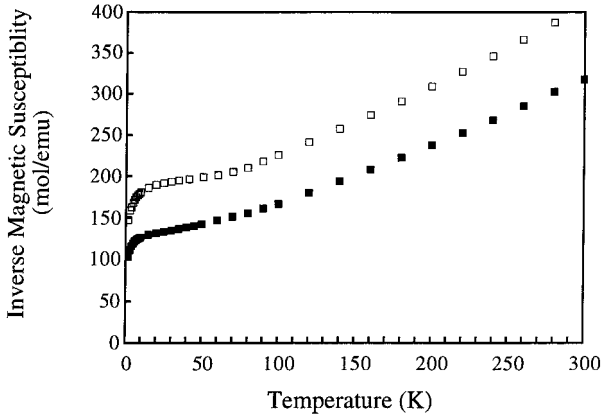

Figure 6. Inverse molar magnetic susceptibility, χ_M (per uranium), of RbU_2SbS_8 (□) and KU_2SbSe_8 (■).

Magnetic susceptibility measurements show Curie−Weiss behavior between 80 and 300 K with μ_{eff} of 3.03 and 3.21 μ_B and θ values of = −160 and −83 K for RbU_2SbS_8 and KU_2SbSe_8, respectively; see Figure 6. These magnetic moments suggest a $5f^2$ electron configuration on U^{4+}. Both crystal field splitting and exchange effects act to reduce the effective moment[19] below the theoretical value for the free ion (3.58 μ_B) using the expression $\mu_{eff} = [J(J + 1)]^{1/2}$ (Russell−Saunders coupling applies).[20] The observed μ_{eff} values of these compounds agree well with those reported for US_3, USe_3, and UTe_3, in which U^{4+} centers are also stabilized in bicapped trigonal prismatic sites.[21] The upward deviation from the linear portion in the $1/\chi_M$ vs T curves,— see Figure 6 below ~70 K for both compounds—is probably due to antiferromagnetic exchange interactions, as suggested by the rather large negative θ values.[22]

The Raman spectrum of RbU_2SbS_8 shows shifts at 236, 281, and 479 cm^{-1} and that of KU_2SbSe_8 shows shifts at 236 and 252 cm^{-1}; see Figure 7. The shift at 479 cm^{-1} for RbU_2SbS_8 and at 252 cm^{-1} for KU_2SbSe_8 are assigned to the stretching vibration of dichalco-

(17) A seesaw coordination is defined as one derived from an octahedral coordination in which two cis-equatorial ligands have been removed.

(18) (a) Grønvold, F.; Drowart, J.; Westrum, E. F., Jr. *The Chemical Thermodynamics of Actinide Elements And Compounds*; International Atomic Energy Agency: Vienna, 1984; pp 161−200 and references therein. (b) Clifton, J. R.; Gruen, D. M.; Ron, A. *J. Chem. Phys.* **1969**, *51*, 224−232. (c) Schoenes, J. *Phys. Rep.* **1980**, *63*, 301−336.

(19) (a) Noel, H.; Troc, R. *J. Solid State Chem.* **1979**, *27*, 123−135. (b) Noël, H. *J. Less Common Met.* **1980**, *72*, 45−49. (c) Dawson, J. K. *J. Chem. Soc.* **1951**, 429−431.

(20) Drago, R. S. *Physical Methods for Chemists*, 2nd ed.; Saunders College Publishing: New York, 1992; pp 480−486.

(21) Freeman, A. J., Darby, J. B., Jr., Eds. *The Actinides: Electronic Structure and Related Properties*; Academic Press: New York, 1974; Vols. I and II.

(22) (a) Suski, W. *J. Solid State Chem.* **1973**, *7*, 385−399. (b) Suski, W. *Phys. Status Solid A* **1972**, *13*, 675−680.

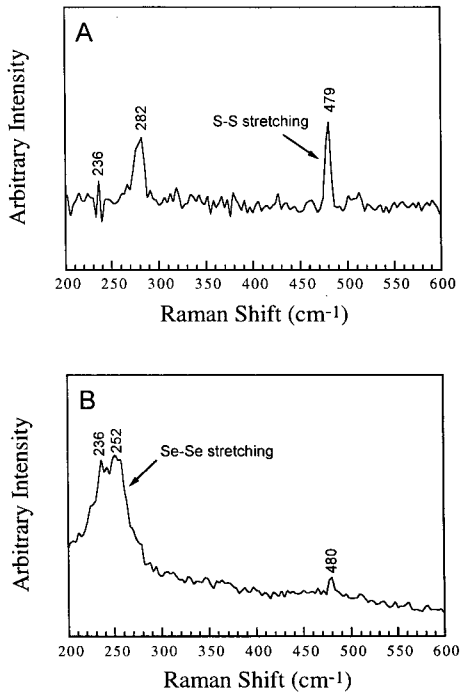

Figure 7. Raman spectra of (A) RbU_2SbS_8 and (B) KU_2SbSe_8.

genide groups and these values are in accord with the S−S/Se−Se stretching frequencies reported for other compounds.[2,23] The weak shift that appears at 480 cm^{-1} in Figure 7B is an overtone. Differential thermal analysis (DTA) showed that both compounds do not melt below 1000 °C.

The presence of f−f transitions eliminate a transparent spectral window in the IR region and limit the possibility that these compounds can be used for nonlinear optics (NLO). However, the RbU_2SbS_8 structure type can potentially be an excellent scaffold for generating NLO materials. For example, if the U^{4+} ions could be substituted with other M^{4+} ions which do not have f or d electrons such as Zr^{4+} and Hf^{4+}, the resulting compounds should be optically transparent below the band gap.

Acknowledgment. Financial support from the Office of Naval Research is gratefully acknowledged. This work made use of the W. M. Keck Microfabrication facility at MSU, a NSF MRSEC facility. The Siemens SMART platform CCD diffractometer was purchased with funds from the National Science Foundation (CHE-9634638). This work made use of the SEM facilities of the Center for Electron Optics at Michigan State University.

Supporting Information Available: Tables of crystallographic details, atomic coordinates, isotropic and anisotropic displacement parameters for all atoms, and interatomic distances and angles for the substructure and the superstructure of RbU_2SbS_8 and KU_2SbSe_8. This material is available free of charge via the Internet at http://pubs.acs.org.

CM990320L

(23) (a) Böttcher, P.; Getzschmann, J.; Keller, R. *Z. Anorg. Allg. Chem.* **1993**, *619*, 476−488. (b) Choi, K.-S.; Patschke, R.; Billinge, S. J. L.; Waner, M. J.; Dantus, M.; Kanatzidis, M. G. *J. Am. Chem. Soc.* **1998**, *120*, 10706−10714.